Geophysical Research Letters

RESEARCH LETTER
10.1029/2020GL090619

The Role of Diabatic Heating in Ferrel Cell Dynamics

Orli Lachmy[1] **and Yohai Kaspi**[2]

[1]Department of Natural Sciences, The Open University of Israel, Ra'anana, Israel, [2]Department of Earth and Planetary Sciences, Weizmann Institute of Science, Rehovot, Israel

Key Points:
- Diabatic heating plays a key role in the midlatitude heat budget controlling the Ferrel cell
- Diabatic heating is concentrated at the Ferrel cell ascending branch during summer and around the Ferrel cell center during winter
- The diabatic heating rate is positively correlated with the wintertime separation between the eddy heat flux and the eddy-driven jet

Supporting Information:
- Supporting Information S1

Correspondence to:
O. Lachmy,
orlila@openu.ac.il

Citation:
Lachmy, O., & Kaspi, Y. (2020). The role of diabatic heating in Ferrel cell dynamics. *Geophysical Research Letters*, *47*, e2020GL090619. https://doi.org/10.1029/2020GL090619

Received 31 AUG 2020
Accepted 18 NOV 2020
Accepted article online 23 NOV 2020

Abstract The Ferrel cell consists of the zonal mean vertical and meridional winds in the midlatitudes. The continuity of the Ferrel circulation and the zonal mean momentum and heat budgets imply a collocation of the eddy-driven jet and poleward eddy heat flux maxima, under certain assumptions, including the negligibility of diabatic heating. The latter assumption is questioned, since midlatitude storms are associated with latent heating in the midtroposphere. In this study, the heat budget of the Ferrel cell in both hemispheres is examined, using the JRA55 reanalysis data set. The diabatic heating rate is significant close to the center of the Ferrel cell during winter and at the ascending branch during summer in both hemispheres. The interannual variability shows a positive correlation between the diabatic heating rate in the midlatitude midtroposphere and the latitudinal separation between the eddy heat flux and the eddy-driven jet maxima during winter in both hemispheres.

Plain Language Summary The midlatitude climate is affected by storms, organized in regions called "storm tracks." Storms are carried eastward by the midlatitude jet stream. The storm track and the jet stream are dynamically coupled, through the heat and momentum budgets. Here we use the heat and momentum budgets, and the continuity of the midlatitude meridional circulation cell, called the "Ferrel cell," to examine the connection between the latitudinal locations of the storm track and jet stream. We focus on the role of diabatic heating by latent heat release in midlatitude storms in the heat budget, and its effect on the circulation. Our analysis shows that the latitudinal separation between the storm track and jet stream increases as the diabatic heating in the midlatitude midtroposphere increases during winter. These results highlight the role of diabatic heating in the midlatitude circulation, which is often overlooked.

1. Introduction

The midlatitude storm tracks are characterized by strong eddy activity and poleward eddy heat flux (EHF) (e.g., Shaw et al., 2016). The midlatitude zonal mean flow includes the jet stream and the Ferrel cell, composed of ascent in high latitudes and descent in the subtropics. The Ferrel cell is primarily eddy driven, in the sense that the vertical motion associated with the Ferrel cell arises mostly from heating and cooling by EHF convergence and divergence. In the absence of nonconservative processes in the free troposphere, the eddy-driven component of the jet (eddy-driven jet, EDJ), the EHF and the Ferrel cell are tightly connected, yet this connection might be modified by the presence of a diabatic heating source.

The EDJ and EHF can be connected through the Eliassen and Palm (EP) flux, which is the flux of wave activity (Eliassen & Palm, 1961). The meridional and vertical components of the EP flux depend on the meridional eddy momentum and heat fluxes, respectively. In the absence of nonlinear and nonconservative processes, the EP flux divergence is zero (e.g., Edmon et al., 1980), which leads to a connection between the EDJ and EHF. The climatological EP flux divergence is mostly positive near the surface and negative in the middle and high troposphere in midlatitudes (e.g., Vallis, 2017), which indicates that nonlinear and nonconservative processes are important, and that a latitudinal separation between the EDJ and EHF is possible. The zonal mean momentum and heat budgets also provide a connection between the EHF, EDJ and Ferrel circulation. The EDJ, identified by surface westerlies, and the poleward EHF are collocated between the descending and ascending branches of the Ferrel cell if diabatic heating and friction are negligible in the free troposphere, and linear friction damps the surface zonal winds (Vallis, 2017). However, when diabatic heating is significant in the midlatitude heat budget, a latitudinal separation between the EDJ and EHF becomes possible, as we demonstrate in this study.

The connection between the latitudes of maximum EDJ and EHF was investigated in several previous studies. Nakamura et al. (2004) showed that the longitudinally dependent EHF and surface westerlies are closely located in both hemispheres. Conversely, Dwyer and O'Gorman (2017) found that the latitude of maximum surface westerlies is a few degrees equatorward of the upward dry EP flux maximum in the lower troposphere, but approximately collocated with the upward moist EP flux, defined using equivalent potential temperature in the EHF term. This highlights the effect of diabatic heating, which is implicit in the moist EP flux, on the latitudinal separation between the EDJ and EHF. The numerical study of Lu et al. (2010) showed that the latitudinal separation between the EDJ and EHF increases as the pole-to-equator temperature difference decreases, yet there is no complete explanation for this dependence.

Here we examine the zonal mean heat budget in winter and summer of the Northern Hemisphere (NH) and Southern Hemisphere (SH), to assess the role of diabatic heating in the midlatitude midtroposphere. We examine the connection between the diabatic heating rate and the latitudinal separation between the EHF and EDJ.

2. Data and Methods

The data are based on the Japanese 55-year Reanalysis (JRA-55) data set (Kobayashi et al., 2015) for the years 1979–2013. The JRA-55 data set includes diabatic heating rates on vertical levels, unlike some of the other leading Reanalysis data sets. The diabatic heating rate presented here is a sum of the following fields: large-scale condensation heating rate, convective heating rate, solar radiative heating rate, longwave radiative heating rate and vertical diffusion heating rate. All the analysis presented here is for data above the surface.

The latitude of maximum value is calculated for the following zonal mean variables in the midlatitudes: (1) midtropospheric EHF; (2) near-surface zonal wind; (3) midtropospheric stream function; (4) near-surface meridional wind; and (5) midtropospheric diabatic heating rate. The latter is used for defining the region over which the diabatic heating rate is averaged. These variables are first vertically integrated, then interpolated to a 0.1° interval grid. The latitude of maximum is the zero crossing of the derivative, calculated by finite differencing. The near-surface zonal and meridional winds are vertically integrated between 800 and 1000 hPa. The EHF, mass stream function and the diabatic heating rate are vertically integrated between 500 and 700 hPa. The latitude of maximum midlatitude diabatic heating is calculated between 40° and 60° for each hemisphere during summer, and between 30° and 50° during winter. The diabatic heating rate is then averaged over a latitudinal range of 5° on each side of its maximum.

3. Results

3.1. The Zonal Mean Heat Budget

In order to assess the role of diabatic heating in the midlatitude circulation, we diagnose the climatological zonal mean heat budget as a function of latitude and pressure (e.g., Holton, 2004, Equation 3.6):

$$\frac{\partial \overline{T}}{\partial t} = -\frac{\overline{v}}{a}\frac{\partial \overline{T}}{\partial \phi} - \overline{\omega}\left(\frac{\partial \overline{T}}{\partial p} - \kappa\frac{\overline{T}}{p}\right) - \frac{1}{a\cos\phi}\frac{\partial\left(\cos\phi\left(\overline{v'T'}\right)\right)}{\partial\phi} - \left(\frac{\partial\left(\overline{\omega'T'}\right)}{\partial p} - \kappa\frac{\left(\overline{\omega'T'}\right)}{p}\right) + \frac{\overline{J}}{c_p}, \quad (1)$$

where T, v, and ω are the temperature, meridional wind and vertical wind in pressure coordinates, respectively, with p being pressure and ϕ latitude. The total diabatic energy tendency is marked by J. The constant c_p is the specific heat capacity of dry air at constant pressure. The constant κ equals R_d/c_p, where R_d is the gas constant of dry air. Earth's radius is given by a. An overbar denotes zonal averaging and prime denotes deviation from the zonal average.

The five terms on the right-hand side of Equation 1, from left to right, represent the meridional temperature advection by the mean flow, the adiabatic term associated with the zonal mean vertical motion (hereafter the "Ferrel cell heating rate"), the meridional EHF convergence, the heating rate by vertical EHF and the diabatic heating rate. The terms on the right-hand side of Equation 1 are shown in Figures 1 and 2, for the midlatitudes of both hemispheres in winter and summer, respectively, except for the meridional temperature advection by the mean flow, which was found to be relatively small. The sum of the diabatic heating rate and the heating rate by vertical EHF is also shown. In the midlatitude midtroposphere (between 500 and

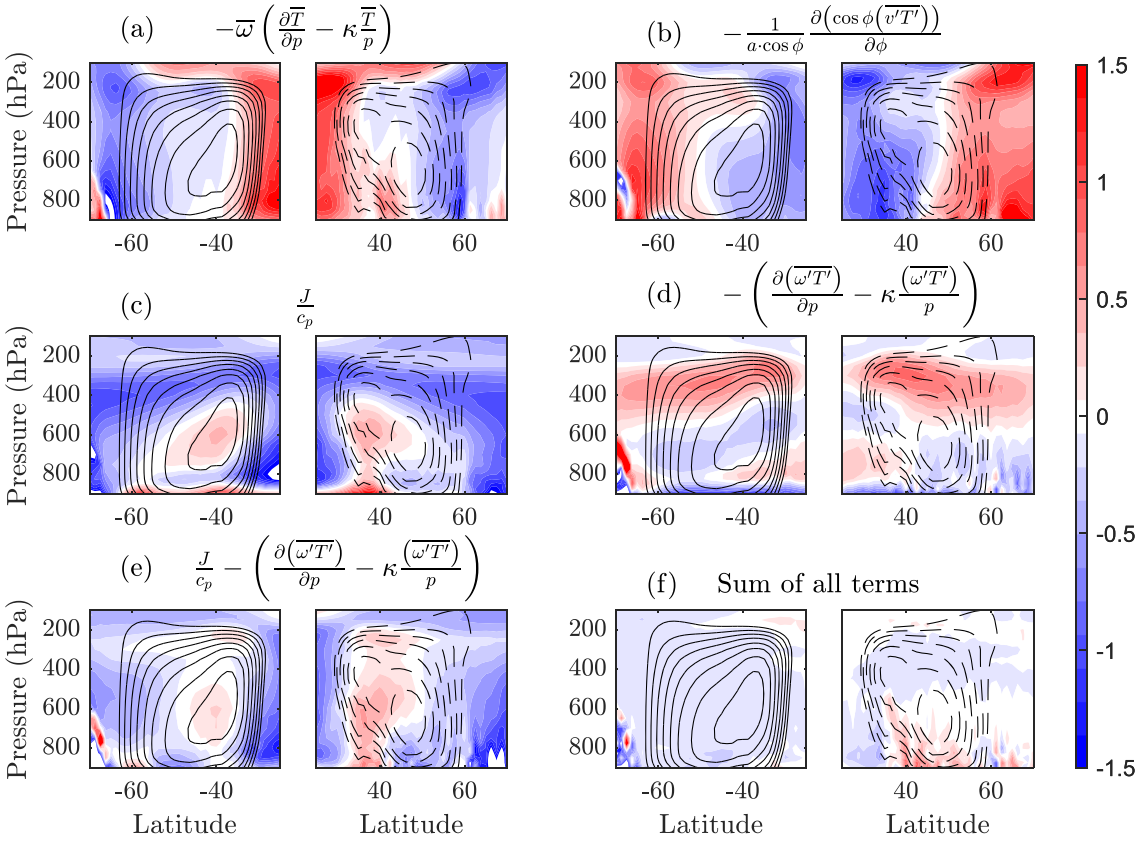

Figure 1. The midlatitude heat budget (shading, in K day^{-1}) and mass stream function (contours) during winter (June–August in the SH and December–February in the NH), based on JRA55 reanalysis for the years 1979–2013. The heat budget terms include: (a) The Ferrel cell heating rate (see text); (b) meridional EHF convergence; (c) diabatic heating rate; (d) heating rate by vertical EHF; (e) sum of the diabatic heating rate and heating rate by vertical EHF; (f) sum of all the terms on the right-hand side of Equation 1. The contour interval for the mass stream function is 5×10^9 kg s^{-1}. Solid and dashed contours indicate positive and negative values, respectively. Only positive (negative) values are shown for the SH (NH) mass stream function.

800 hPa) this sum is dominated by the diabatic heating term (Figures 1c and 1e, and 2c and 2e). The sum of all the terms on the right-hand side of Equation 1 (including the meridional temperature advection by the mean flow) is negligible in the midlatitude midtroposphere, indicating that the balance is closed (Figures 1f and 2f). The midlatitude midtropospheric climatological winter and summer heat budgets can therefore be approximated by

$$\overline{\omega}\left(\frac{\partial\overline{T}}{\partial p}-\kappa\frac{\overline{T}}{p}\right)=-\frac{1}{a\cos\phi}\frac{\partial\left(\cos\phi\left(\overline{v'T'}\right)\right)}{\partial\phi}+\frac{\overline{J}}{c_p}, \tag{2}$$

where the temperature tendency, the meridional temperature advection by the mean flow and the heating rate by vertical EHF are neglected.

The meridional mass stream function, Ψ, of the Ferrel cell is also shown in Figures 1 and 2. The stream function Ψ is defined such that

$$\overline{v}=\frac{g}{2\pi a\cos\phi}\frac{\partial\Psi}{\partial p},\ \overline{\omega}=-\frac{g}{2\pi a^2\cos\phi}\frac{\partial\Psi}{\partial\phi}, \tag{3}$$

where g is Earth's gravitational acceleration.

While the Ferrel cell heating rate (Figures 1a and 2a) and the meridional EHF convergence (Figures 1b and 2b) approximately balance each other at the flanks of the Ferrel cell, the diabatic heating rate is important near the center of the Ferrel cell during winter (Figure 1c) and at the ascending branch of the Ferrel cell during summer (Figure 2c). We note that the structure of the diabatic heating rate in the midlatitude midtroposphere is determined mostly by latent heating from large scale condensation, while radiative cooling

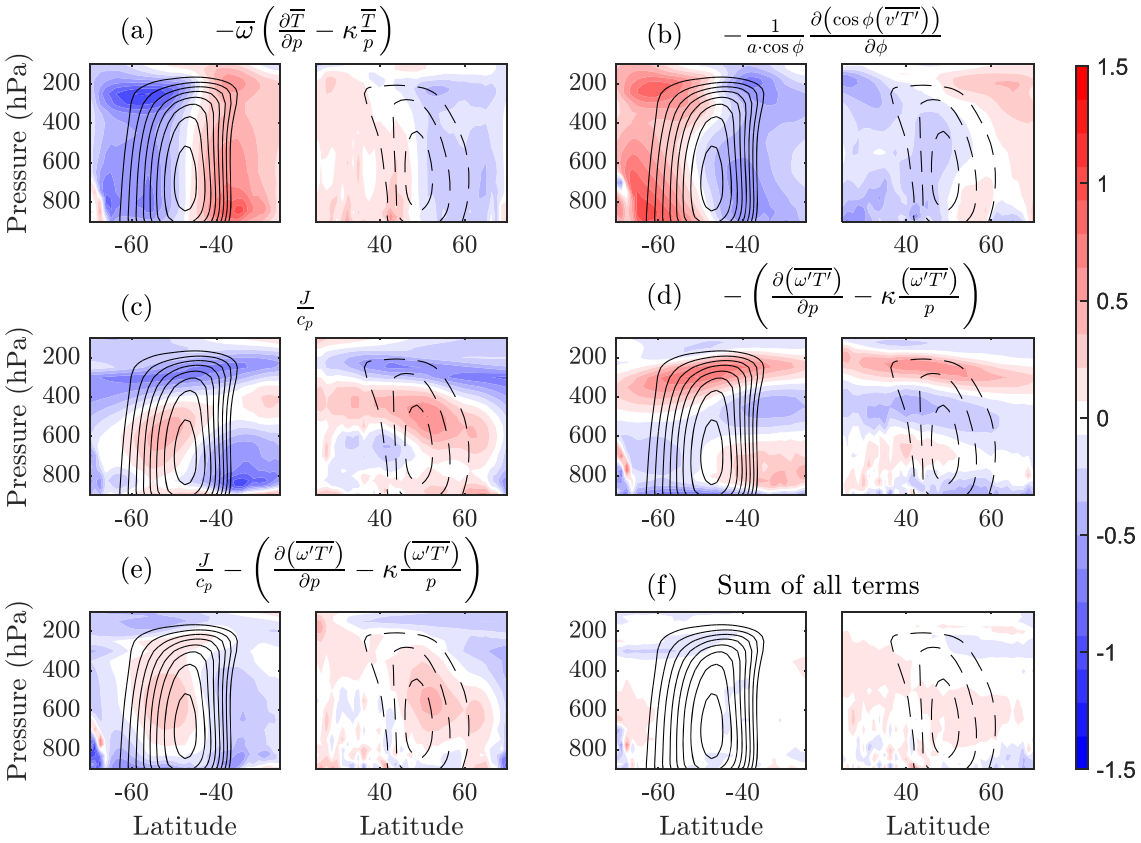

Figure 2. Similar to Figure 1, but for summer (December–February in the SH and June–August in the NH).

is relatively uniform in this region (not shown). The seasonal difference in the location of the diabatic heating maximum relative to the Ferrel circulation is likely related to the different types of convection during winter and summer (e.g., Catto et al., 2012; Pfahl et al., 2014).

3.2. The Latitudinal Separation Between the Eddy-Driven Jet and EHF

3.2.1. Theoretical Reasoning

The connection between the latitudes of the EDJ and EHF can be derived from the heat and momentum budgets, as we show next. In what follows we refer to the area-weighted zonal mean of the poleward EHF, $|\cos\phi\left(\overline{v'T'}\right)|$, as EHF. According to Equation 2, if the diabatic heating is neglected, the maximum EHF would be located between the descending and ascending branches of the Ferrel cell, where ω is zero. According to Equation 3, the latitude where $\omega = 0$ is the latitude of maximum $|\Psi|$. Therefore, if the diabatic heating is negligible in the midlatitude midtroposphere, then the latitudes of maximum EHF and maximum $|\Psi|$ are collocated in this region.

The structure of the Ferrel cell is related also to the latitude of the EDJ. The surface westerlies are proportional to the vertically integrated eddy momentum flux convergence and mark the location of the EDJ. Near the surface, the zonal mean zonal momentum balance can be approximated by (Vallis, 2017):

$$f\overline{v_s} = r\overline{u_s}, \tag{4}$$

where f is the Coriolis parameter, r is a constant linear drag coefficient and the subscript s denotes surface values. We refer to the latitude of maximum area-weighted zonal mean surface westerlies, $\cos\phi\,\overline{u_s}$, as the latitude of the EDJ. According to Equation 4, the latitude of the EDJ, is approximately collocated with the maximum area-weighted zonal mean of the poleward surface wind, $|\cos\phi\overline{v_s}|$, if the meridional derivative of f is neglected. According to Equation 3, if the structure of the stream function is not tilted with pressure (i.e., the latitude of maximum $|\Psi|$ is the same for all pressure levels in the Ferrel cell), then the latitudes of maximum $|\cos\phi\overline{v_s}|$ and maximum midlatitude midtropospheric $|\Psi|$ are collocated.

Based on the above reasoning, the EDJ and EHF maxima would be collocated if all the following conditions are satisfied:

1. The maxima of midtropospheric EHF and $|\Psi|$ are collocated.
2. The maxima of midtropospheric $|\Psi|$ and $|\cos\phi\overline{v}_s|$ are collocated.
3. The maxima of $|\cos\phi\overline{v}_s|$ and EDJ are collocated.

Since diabatic heating is significant in the midlatitude midtropospheric heat budget, the first condition might not be satisfied, which could allow for a separation between the EDJ and EHF maxima. We examine this possibility next.

3.2.2. Interannual Variability

In order to examine the role of diabatic heating in the midlatitude circulation, we analyze the interannual variability of the latitudinal separation between the EDJ and EHF in the SH and NH winter and summer, and its relation to the validity of the above conditions (Figure 3). During NH summer, the EHF is maximal between 50°N and 60°N, 2.5–16° poleward of the EDJ (red triangles in Figure 3a). During SH summer, the EHF is also poleward of the EDJ in most years, but the separation is only 0–4° (blue circles in Figure 3a). During NH winter, the EHF is maximal between 45°N and 50°N, while the EDJ latitude varies between 34°N and 47°N (orange triangles in Figure 3b). During SH winter, the EHF is maximal between 47°S and 51°S, while the EDJ latitude is between 40°S and 53°S (green circles in Figure 3b). While the EHF is maximal poleward of the EDJ in most years during both summer and winter in both hemispheres, the latitudinal separation is larger in the NH than in the SH and larger during winter than summer. The relation between the latitudes of maximum EHF and EDJ is approximately linear during SH summer (Figure 3a), whereas during SH winter, the latitude of maximum EHF is approximately constant, independent of the latitude of maximum EDJ (Figure 3b). Next we examine the conditions for the latitudinal separation between the EHF and EDJ.

Condition (1) above is examined in Figures 3c and 3d. During summer in both hemispheres, the maximum of the EHF is poleward of the maximum $|\Psi|$, and the relation between them is approximately linear. The separation between the two maxima is less than 7°, for all the years in the data set, except for three NH summers (Figure 3c). During NH winter, the separation between the maxima of EHF and $|\Psi|$ is less than 5° for 31 out of the 35 years in the data set (Figure 3d). During SH winter, the EHF is maximal 0–14° poleward of $|\Psi|$. The large separation between the EHF and $|\Psi|$ during SH winter implies that diabatic heating is significant in the midlatitude midtropospheric heat budget in this season.

Condition (2) above is examined in Figures 3e and 3f. During summer in both hemispheres, $|\Psi|$ and $|\cos\phi\overline{v}_s|$ are approximately collocated (Figure 3e). In contrast, during winter, the maximum of $|\Psi|$ is equatorward of the maximum of $|\cos\phi\overline{v}_s|$ for most years in the data set (Figure 3f), consistent with the structure of the Ferrel cell stream function during winter, which is tilted equatorward with height (Figures 1 and 2). However, the separation between the maxima of $|\Psi|$ and $|\cos\phi\overline{v}_s|$ does not explain the separation between the EHF and EDJ during winter, since the maximum of $|\Psi|$ is equatorward of the maximum $|\cos\phi\overline{v}_s|$, while the maximum of the EHF is poleward of the maximum EDJ (Figures 3b and 3f).

Condition (3) above is examined in Figures 3g and 3h. During the SH summer the maxima of $|\cos\phi\overline{v}_s|$ and EDJ are approximately collocated. During the NH summer, the $|\cos\phi\overline{v}_s|$ maximum is 0–9° poleward of the EDJ maximum (Figure 3g). During the SH winter, the latitudinal separation between $|\cos\phi\overline{v}_s|$ and EDJ is less than 3° for 28 out of the 35 years in the data set (Figure 3h). During the NH winter, the difference between the latitudes of maximum $|\cos\phi\overline{v}_s|$ and EDJ is 1–6°. The large latitudinal separation between the maxima of $|\cos\phi\overline{v}_s|$ and the EDJ in the NH shows that the approximation of linear surface drag (Equation 4) might be inaccurate there, perhaps because of the Tibetan Plateau.

These results show that all three conditions for the collocation of the EDJ and EHF are approximately satisfied in the SH summer, while Conditions (1) and (3) are less accurate in the NH summer, and none of the conditions are satisfied during winter in both hemispheres, except for Condition (3), which is satisfied during most SH winters. This is consistent with the collocation of the EDJ and EHF in the SH summer, and their large separation during winter in both hemispheres. The latter is partially due to the tilted structure of Ψ during winter, affecting Condition (2), and partially due to the diabatic heating being significant in the midlatitude midtropospheric heat budget, affecting Condition (1). In the NH winter, the deviation of the

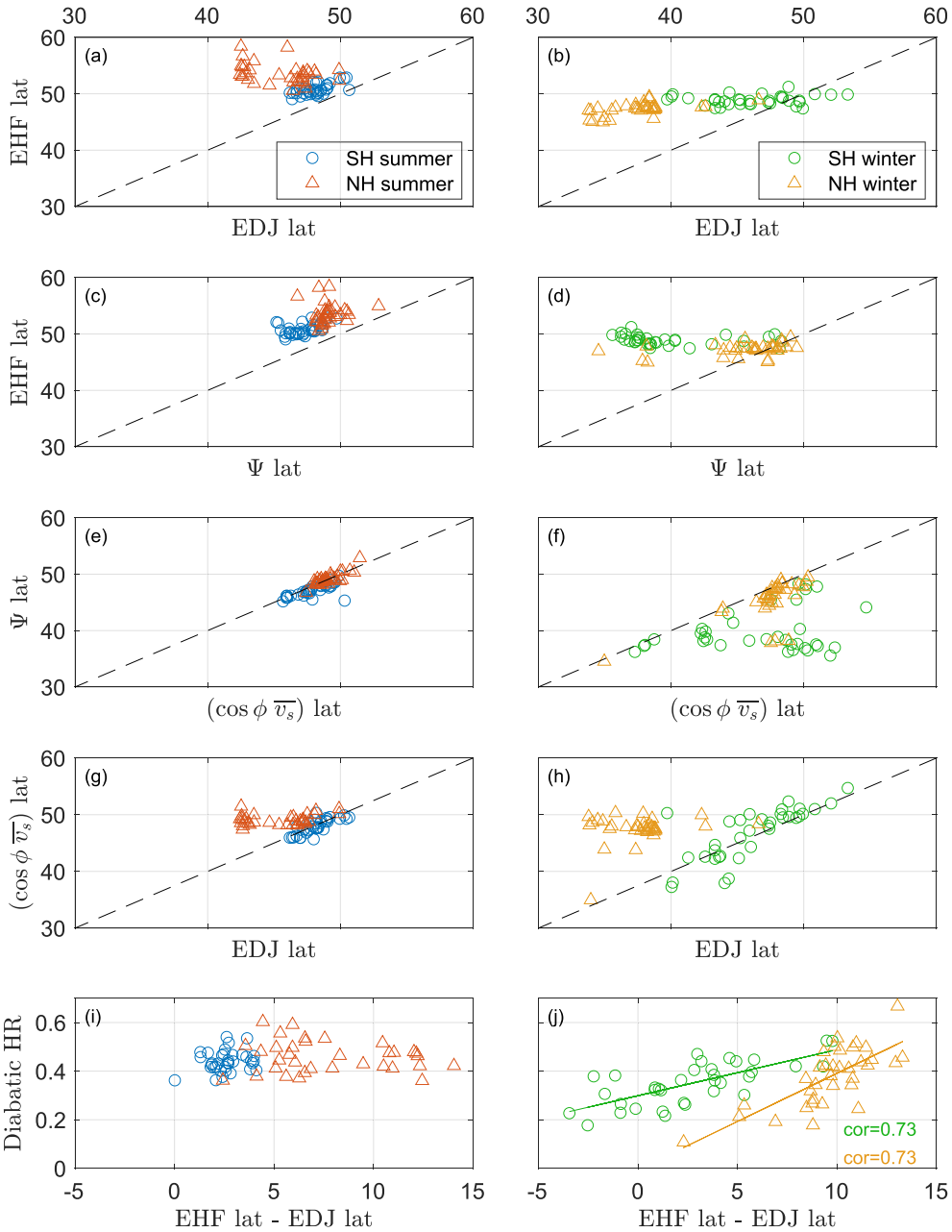

Figure 3. Scatter diagram showing the interannual variability of the latitudinal separation between the EHF and EDJ and its relation with diabatic heating and other variables. The latitudes of maximum (a, b) EHF versus EDJ, (c, d), EHF versus midtropospheric $|\Psi|$, (e, f) midtropospheric $|\Psi|$ versus poleward surface wind ($|\cos\phi\overline{v_s}|$), (g, h), $|\cos\phi\overline{v_s}|$ versus EDJ, and (i, j) mean diabatic heating rate in the midlatitude midtroposphere and the latitudinal separation between the EHF and EDJ. Each marker is for a specific year and season (the seasons are defined as in Figures 1 and 2). Blue circles and red triangles in (a), (c), (e), (g), and (i) mark the SH summer and NH summer, respectively. Green circles and orange triangles in (b), (d), (f), (h), and (j) mark the SH winter and NH winter, respectively. Latitudes in the SH are multiplied by (−1) for convenience. The black dashed line in (a)–(h) marks the one-to-one slope. The green and orange lines in (j) show the linear fit for the data from the SH winter and NH winter, respectively. The correlation coefficients for the respective season are also shown in (j).

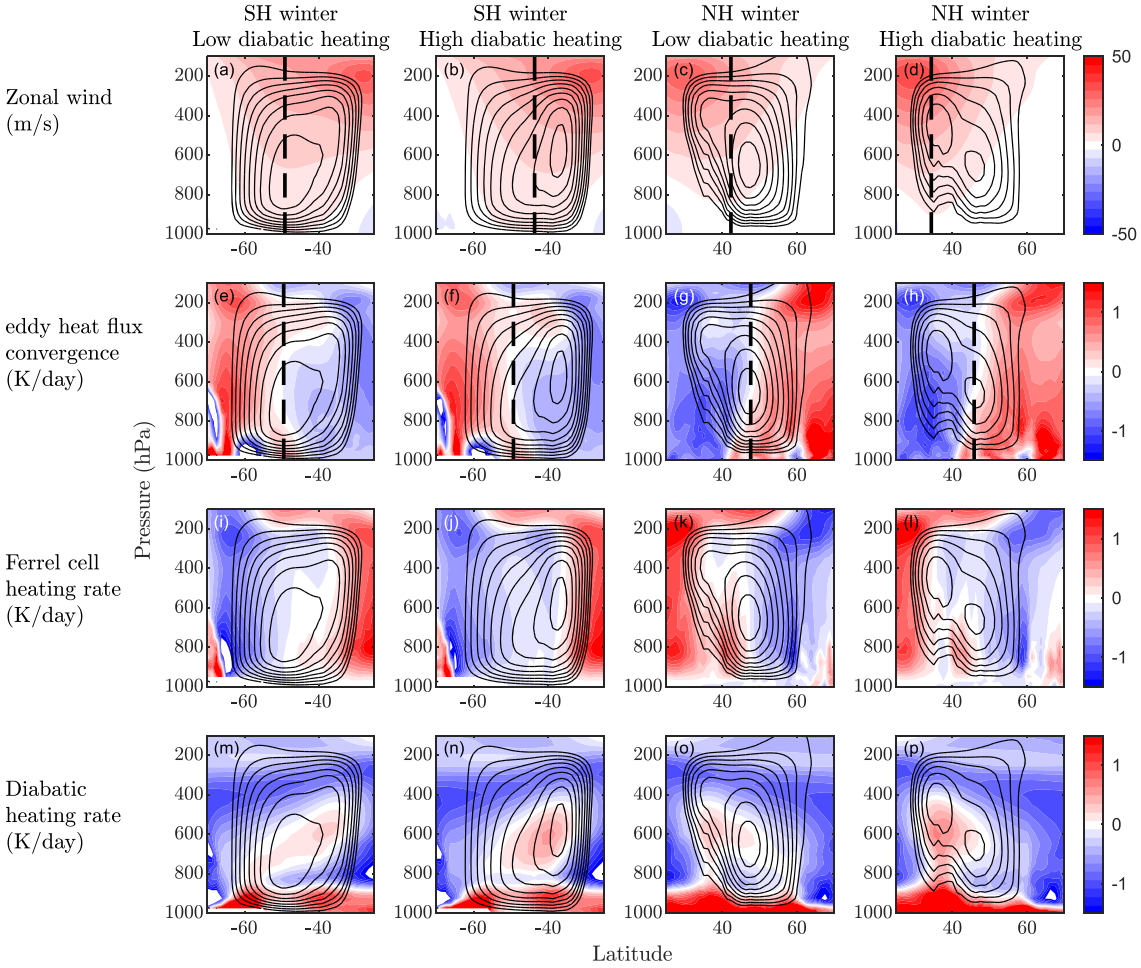

Figure 4. Composites of midlatitude circulation variables, based on diabatic heating rates in the midlatitude midtroposphere. The SH and NH winter composites are shown in the two left and right columns, respectively. The shading shows (a–d) zonal mean zonal wind in m s^{-1}; (e–h) EHF convergence in K day^{-1}; (i–l) Ferrel cell heating rate (see text) in K day^{-1}; and (m–p) diabatic heating rate in K day^{-1}. Contours show the Ferrel cell mass stream function, with a contour interval of 5×10^9 kg s^{-1}. For convenience, the mass stream function in the NH is multiplied by (−1) and only positive values are shown. The vertical dashed lines in (a)–(d) and (e)–(h) mark the latitudes of maximum EDJ and EHF, respectively.

surface momentum budget from Equation 4 also contributes to the latitudinal separation between the EDJ and EHF.

The role of diabatic heating in the latitudinal separation between the EDJ and EHF during winter can be assessed by looking at the interannual variability of the midlatitude midtropospheric diabatic heating rate, against the latitudinal separation between the EHF and EDJ (Figures 3i and 3j). The correlation between these variables is not significant during summer in both hemispheres but is equal to 0.73 during winter in both hemispheres (Figure 3h), implying that the large separation between the EHF and EDJ in certain years during winter is related to high diabatic heating rates in the midlatitude midtroposphere. The larger separation during winters with high diabatic heating rates is mostly due to an equatorward shift of the EDJ (supporting information Figure S1), while the EHF latitude is nearly constant (Figure 3b).

In order to gain insight for the connection between the diabatic heating rate and the latitudinal separation between the EHF and EDJ, we examine the circulation for composites of years with low and high diabatic heating rates during winter in each hemisphere (Figure 4). The threshold for low (high) diabatic heating rate is one standard deviation below (above) the multiannual winter mean. In the low diabatic heating rate composite of SH winters, the EDJ and EHF maxima are collocated around latitude 49°S (Figures 4a and 4e). EHF convergence balances the adiabatic cooling by the Ferrel cell ascending branch poleward of the maximum stream function (Figures 4e and 4i), and the structure of the stream function is relatively

symmetric around its maximum (Figures 4a, 4e, 4i, and 4m). This composite is close to satisfying all three conditions for the collocation of the EHF and EDJ maxima.

In the high diabatic heating rate composite of SH winters, the EDJ maximum is around 44°S, while the EHF maximum is around 49°S (Figures 4b and 4f). The maximum stream function is around 37°S, and the ascending branch of the Ferrel cell is much wider than the descending branch, as seen from the structure of the stream function and from the Ferrel cell heating rate (Figure 4j). Between 37°S and 49°S, diabatic heating is balanced by adiabatic cooling by the ascending branch of the Ferrel cell and EHF divergence (Figures 4f, 4j, and 4n). Poleward of 49°S, cooling by the Ferrel cell ascending branch is balanced mainly by EHF convergence. The strong diabatic heating is clearly related to the highly asymmetric structure of the Ferrel cell, through the heat balance, and enables the situation where the EHF maximum is far poleward of the maximum stream function and EDJ.

In the NH winter, the difference in the circulation between years with low and high diabatic heating rate has some common features with the difference seen in the SH winter. In the low diabatic heating rate composite of NH winters, the EDJ and EHF are closer, and the structure of the Ferrel cell stream function is more symmetric than in the high diabatic heating rate composite (Figures 4c, 4d, 4g, and 4h). The differences in the heat budget between NH winters with low and high diabatic heating rate are mostly apparent in the midtroposphere (between 700 and 400 hPa) between latitudes 35°N and 45°. In the low diabatic heating rate composite, this region is part of the descending branch of the Ferrel cell, which leads to a positive Ferrel cell heating rate (Figure 4k) that balances the EHF divergence (Figure 4g) and the weak diabatic heating (Figure 4o). In the high diabatic heating rate composite, this region is mostly within the ascending branch, as seen by the negative Ferrel cell heating rate (Figure 4l). The negative Ferrel cell heating rate and the EHF divergence in this region (Figure 4h) are balanced by the strong diabatic heating (Figure 4p). In the NH winter, as in the SH winter, strong diabatic heating in the midlatitude midtroposphere in certain years enables a latitudinal separation between the region of maximum stream function, where the EDJ is located, and the region of maximum EHF, while maintaining the heat balance between the Ferrel cell heating rate, the EHF convergence and the diabatic heating rate.

4. Conclusions

The role of diabatic heating in the midlatitude heat budget and circulation is often ignored in theoretical studies (e.g., Vallis, 2017), leading to the conclusion that the EHF and EDJ are collocated, if the structure of the Ferrel cell stream function is not tilted with height, and the near-surface Coriolis force is balanced by linear drag. Using the JRA55 reanalysis data set for years 1979–2013, we show that diabatic heating is a significant term in the midlatitude midtropospheric heat budget, compensating for imbalances between the adiabatic heating rate associated with the Ferrel cell vertical motion and the EHF convergence. The climatological heat budget shows significant diabatic heating at the ascending branch of the Ferrel cell during summer in both hemispheres, and near the center of the Ferrel cell during winter in both hemispheres (Figures 1 and 2). Analyzing the interannual variability of the circulation, we obtain the following results:

- During the SH summer, the conditions for the collocation of the EHF and EDJ maxima are approximately satisfied and the maxima of EDJ and EHF are nearly collocated. During the NH summer, the EHF is maximal poleward of the EDJ, possibly due to topography.
- During winter in both hemispheres the conditions for the collocation of the EHF and EDJ maxima are not satisfied, except for specific years. This is related to the wintertime meridional tilt of the Ferrel cell with height and to the role of diabatic heating in the heat budget.
- Diabatic heating in the midlatitude midtroposphere is positively correlated with the latitudinal separation between the EDJ and EHF during winter in both hemispheres (Figure 3j). During winters with strong diabatic heating, the Ferrel cell stream function maximum is shifted equatorward, while the maximum EHF latitude remains approximately constant. This allows for a separation between the EHF and the EDJ (Figure 4).

The relation we find here between strong midlatitude diabatic heating and an equatorward shift of the EDJ, on interannual time scales, is consistent with previous studies, which examined the relation between the annular modes and latent heat release in the midlatitudes on daily to monthly time scales. The northern and southern annular modes are the dominant variability modes of the zonal mean midlatitude circulation,

which describe latitudinal shifts of the EDJ (Thompson & Wallace, 2000). Several studies found that during the positive phase of the annular mode, when the EDJ is displaced poleward, latent heating decreases at midlatitudes and increases at high latitudes (Boer et al., 2001; Kidston et al., 2010; Yamada & Pauluis, 2015). Yamada and Pauluis (2015) showed that the poleward shift of the midlatitude latent heating during the positive phase of the annular mode is due to the poleward shift of the Ferrel cell and the associated moisture transport. Whether a similar mechanism affects interannual variations in midlatitude diabatic heating remains a topic for future study.

Data Availability Statement

The JRA55 reanalysis data (Japan Meteorological Agency, J., 2013) can be downloaded from the Research Data Archive at the National Center for Atmospheric Research, Computational and Information Systems Laboratory (https://doi.org/10.5065/D6HH6H41).

Acknowledgments
The authors thank two anonymous reviewers for their useful comments. This research was supported by the Israel Science Foundation (grants Nos. 1658/18 and 996/20). The authors are grateful to the Japanese Meteorological Agency for providing the JRA55 reanalysis (Kobayashi et al., 2015).

References

Boer, G. J., Fourest, S., & Yu, B. (2001). The signature of the annular modes in the moisture budget. *Journal of Climate*, *14*, 3655–3665.
Catto, J. L., Jakob, C., Berry, G., & Nicholls, N. (2012). Relating global precipitation to atmospheric fronts. *Geophysical Research Letters*, *39*, L10805. https://doi.org/10.1029/2012GL051736
Dwyer, J. G., & O'Gorman, P. A. (2017). Moist formulations of the Eliassen–Palm flux and their connection to the surface westerlies. *Journal of the Atmospheric Sciences*, *74*, 513–530.
Edmon, H. J., Hoskins, B. J., & McIntyre, M. E. (1980). Eliassen-Palm cross sections for the troposphere. *Journal of the Atmospheric Sciences*, *37*, 2600–2616.
Eliassen, A., & Palm, E. (1961). On the transfer of energy in stationary mountain waves. *Geofysiske Publikasjoner*, *22*, 1–23.
Holton, J. R. (2004). *An introduction to dynamic meteorology*. San Diego, New York: Elsevier Academic Press.
Japan Meteorological Agency, J. (2013). JRA-55: Japanese 55-year reanalysis, daily 3-hourly and 6-hourly data. https://doi.org/10.5065/D6HH6H41
Kidston, J., Frierson, D. M. W., Renwick, J. A., & Vallis, G. K. (2010). Observations, simulations, and dynamics of jet stream variability and annular modes. *Journal of Climate*, *23*, 6186–6199.
Kobayashi, S., Ota, Y., Harada, Y., Ebita, A., Moriya, M., Onoda, H., et al. (2015). The JRA-55 reanalysis: General specifications and basic characteristics. *Journal of the Meteorological Society of Japan*, *93*(1), 5–48.
Lu, J., Chen, G., & Frierson, D. M. W. (2010). The position of the midlatitude storm track and eddy-driven westerlies in aquaplanet AGCMs. *Journal of the Atmospheric Sciences*, *67*, 3984–4000.
Nakamura, H., Sampe, T., Tanimoto, Y., & Shimpo, A. (2004). Observed associations among storm tracks, jet streams and midlatitude oceanic fronts. *The Earth's Climate: The Ocean-Atmosphere Interaction Geophysical Monograph*, *147*, 329–345.
Pfahl, S., Madonna, E., Boettcher, M., Joos, H., & Wernli, H. (2014). Warm conveyor belts in the ERA-Interim dataset (1979–2010). Part II: Moisture origin and relevance for precipitation. *Journal of Climate*, *27*, 27–40.
Shaw, T. A., Baldwin, M., Barnes, E. A., Caballero, R., Garfinkel, C. I., Hwang, Y.-T., et al. (2016). Storm track processes and the opposing influences of climate change. *Nature Geoscience*, *9*, 656–664.
Thompson, D. W. J., & Wallace, J. M. (2000). Annular modes in the extratropical circulation. Part I: Month-to-month variability. *Journal of Climate*, *13*, 1000–1016.
Vallis, G. K. (2017). *Atmospheric and oceanic fluid dynamics*. Cambridge: Cambridge University Press.
Yamada, R., & Pauluis, O. (2015). Annular mode variability of the atmospheric meridional energy transport and circulation. *Journal of the Atmospheric Sciences*, *72*, 2070–2089.